2006

The Theory of a Scroll Profile

Hubert Bukac
Little Dynamics

THE THEORY OF SCROLL PROFILE

Hubert Bukac
Little Dynamics, Inc., 21 County Road 1238, Vinemont, AL 35179-6301
Tel.: (256) 775-2871, E-mail: hbukac@littledynamics.com

ABSTRACT

Only a pair of parallel curves can create a pocket that compresses gas. A review of theory of parallel curves that is presented here shows that there is more general way how to design an arbitrary scroll profile. Several selected types of plane spirals are discussed here. A common way of creating a curve that is parallel with a given involute of a circle is to rotate the given involute of a circle plus or minus one hundred eighty degrees, but this is not possible for all types of spirals. The same parallel curve can be generated by application of equations of parallel curves.

1. INTRODUCTION

Although, the involute of a circle is the most frequently used type of scroll profile, there exist other types of plane spirals that can be used to generate alternative scroll profiles. The necessary condition for a pair of spirals to create a pocket that can compress gas is to form a pair of parallel curves. These curves are also known as Bertrand curves (Bertrand Joseph, 1830-1900, French mathematician). An infinite number of parallel curves can be generated from a given plane curve, but not every spatial curve may have a parallel curve. In most papers on the theory of scroll profile, the authors start with vector form of intrinsic equation, where the coordinate is the trajectory, the path. Such a concise notation is not very useful for a practicing engineer. This paper skips this type of generalization and rather than that it starts with parametric equations of a spiral in the x-y system of coordinates. It is shown that an involute of a circle that is rotated $\pm\pi$ is actually a parallel curve that is parallel with the given involute of a circle. Some spirals can achieve higher compression ratio in the same space than the other ones. Each type of spiral has specific properties that can also affect noise and vibration of a scroll compressor. These properties are more important for radially compliant scroll compressors rather than for the fixed-orbiting-radius scroll compressors.

2. PARALLEL CURVES

Two curves $\mathbf{r}=\mathbf{r}(s)$, and $\bar{\mathbf{r}}=\bar{\mathbf{r}}(s)$ form a pair of parallel curves if

$$\bar{\mathbf{r}}(s)=\mathbf{r}(s)+c\cdot\mathbf{n}(s) \tag{1}$$

Where

$\mathbf{r}(s)$	is original curve
$\bar{\mathbf{r}}(s)$	is parallel curve
$\mathbf{n}(s)$	is a normal of the curve
s	is the natural coordinate of the curve, the length of the arc of curve [m]
c	is an arbitrary constant, positive or negative [m]

The above concise vector notation (1) is of a little practical use. More practical is the notation in the Cartesian system of coordinates.

A plane-curve that has parametric equations $x=\varphi(t)$, $y=\psi(t)$ has a corresponding parallel curve, which equations are

$$\bar{x}=\varphi(t)+c\cdot\frac{\psi'(t)}{\sqrt{\varphi'^2(t)+\psi'^2(t)}} \tag{2}$$

$$\bar{y} = \psi(t) - c \cdot \frac{\varphi'(t)}{\sqrt{\varphi'^2(t) + \psi'^2(t)}} \tag{3}$$

In the equations (2) and (3) the dash indicates derivative by the parameter. Fig. 1 shows two parallel curves k and $\bar{k}$

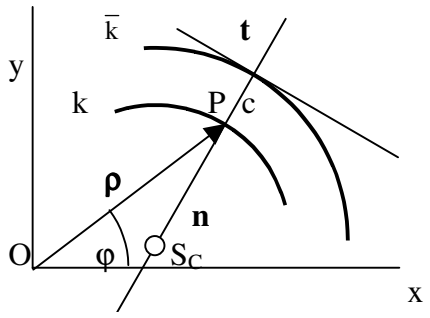

Fig. 1: Formation of two parallel curves

If we express location of point P in Fig. 1 by means of radius vector $\boldsymbol{\rho}$ and angle φ, equations (2) and (3) will take the form

$$\bar{x} = \rho \cdot \cos\varphi + c \cdot \frac{\rho' \cdot \sin\varphi + \rho \cdot \cos\varphi}{\sqrt{\rho'^2 + \rho^2}} \tag{2a}$$

$$\bar{y} = \rho \cdot \sin\rho - c \cdot \frac{\rho' \cdot \cos\rho - \rho \cdot \sin\rho}{\sqrt{\rho'^2 + \rho^2}} \tag{3a}$$

In some cases, it may be more convenient to use equations (2a) and (3a) rather than equations (2) and (3).

In the case of a spiral, the maximum theoretical distance between parallel spirals cannot be arbitrarily long. As we can be see in Fig. 1, the maximum possible orbiting radius R_{OR} is equal to c. If the innermost tip of the vane has thickness s_o[m] then the orbiting radius is $R_{OR} = c - s_o$.

$$c = \frac{1}{2} \cdot \sqrt{\left[x(\varphi_0 + 2\cdot\pi) - x(\varphi_0)\right]^2 + \left[y(\varphi_0 + 2\cdot\pi) - y(\varphi_0)\right]^2} \tag{4}$$

Where

φ_0 is beginning angle [rad]
R_{OR} is orbiting radius [m]

As a case study, we will show geometry of a scroll profile generated by a power spiral. The length ρ of radius vector of a power spiral increases with the power of the parameter φ. Thus, the radius vector of a power spiral is

$$\rho = a \cdot \varphi^b \tag{5}$$

Where

a is an arbitrary constant, a>0, [m]
b is exponent, it is a constant

Three special values of b in equation (5) define three types of commonly known spirals. Thus, if b = 0 the spiral degenerates into a circle; if b = 1, equation (5) defines the spiral of Archimedes; if b =-1, equation (5) defines a hyperbolic spiral.

The parametric equations of a power spiral are

$$x = a \cdot \varphi^b \cdot \cos\varphi \tag{6}$$

$$y = a \cdot \varphi^b \cdot \sin\varphi \tag{7}$$

When we substitute equations (6) and (7) and their derivatives into equations (2) and (3), we get governing equations of a parallel power spiral. Fig. 2 shows an example of parallel power spirals and creation of a pocket.

$$\bar{x} = x + c \cdot \frac{\left(\frac{b}{\varphi}\right) \cdot \sin\varphi + \cos\varphi}{\sqrt{\left(\frac{b}{\varphi}\right)^2 + 1}} \tag{8}$$

$$\bar{y} = y - c \cdot \frac{\left(\frac{b}{\varphi}\right) \cdot \cos\varphi - \sin\varphi}{\sqrt{\left(\frac{b}{\varphi}\right)^2 + 1}} \tag{9}$$

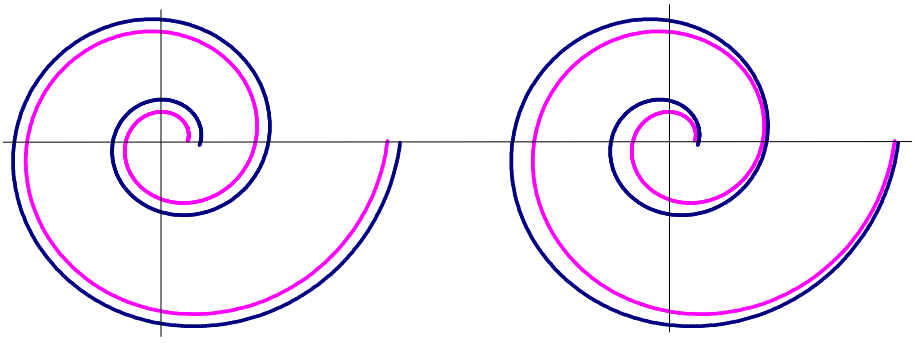

Fig. 2: Parallel power spirals and creation of a pocket

2.1 Creating Vanes

We can see, in the Fig. 2, the original power spiral makes a wall of one vane while the parallel one makes wall of the other vane. Each spiral represents actually a surface of fixed and orbiting scroll.

In order to make further calculations simpler, we start with the spiral that is the centerline of the gap between fixed and orbiting scrolls. Fig. 2 shows that a single spiral can generate only pocket on one side. However, we need another pocket that is symmetrical with the first one. We can achieve that by creating a mirror image of the first centerline. The first centerline has the equations

$$x_1 = \rho \cdot \varphi^b \cdot \cos\varphi \tag{10}$$

$$y_1 = \rho \cdot \varphi^b \cdot \sin\varphi \tag{11}$$

Where

x_1 is x-coordinate of the first centerline [m]
y_1 is y-coordinate of the first centerline [m]

The second centerline that is a mirror image of the first one has the equations

$$x_2 = -\rho \cdot \varphi^b \cdot \cos\varphi \tag{12}$$

$$y_2 = -\rho \cdot \varphi^b \cdot \sin\varphi \tag{13}$$

Where

x_2 is x-coordinate of the first centerline [m]
y_1 is y-coordinate of the first centerline [m]

The parallel curve that forms the outer wall of the first gap has the equation

$$x_{11} = \left(x_1 + \frac{c}{2} \cdot \frac{\left(\frac{b}{\varphi}\right) \cdot \sin\varphi + \cos\varphi}{\sqrt{\left(\frac{b}{\varphi}\right)^2 + 1}} \right) \tag{14}$$

$$y_{11} = \left(y_1 - \frac{c}{2} \cdot \frac{\left(\frac{b}{\varphi}\right) \cdot \cos\varphi - \sin\varphi}{\sqrt{\left(\frac{b}{\varphi}\right)^2 + 1}} \right) \tag{15}$$

Where

x_{11} is x-coordinate of the outer wall of the first gap [m]

y_{11} is y-coordinate of the outer wall of the first gap [m]

The parallel curve that forms the inner wall of the first gap has the equations

$$x_{12} = \left(x_1 - \frac{c}{2} \cdot \frac{\left(\frac{b}{\varphi}\right) \cdot \sin\varphi + \cos\varphi}{\sqrt{\left(\frac{b}{\varphi}\right)^2 + 1}} \right) \tag{16}$$

$$y_{12} = \left(y_1 + \frac{c}{2} \cdot \frac{\left(\frac{b}{\varphi}\right) \cdot \cos\varphi - \sin\varphi}{\sqrt{\left(\frac{b}{\varphi}\right)^2 + 1}} \right) \tag{17}$$

Where

x_{12} is x-coordinate of the inner wall of the first gap [m]

y_{12} is x-coordinate of the inner wall of the first gap [m]

The outer wall of the second (mirror image) gap has the equations

$$x_{21} = \left(x_2 + \frac{c}{2} \cdot \frac{\left(\frac{b}{\varphi}\right) \cdot \sin\varphi + \cos\varphi}{\sqrt{\left(\frac{b}{\varphi}\right)^2 + 1}} \right) \tag{18}$$

$$y_{21} = \left(y_2 - \frac{c}{2} \cdot \frac{\left(\frac{b}{\varphi}\right) \cdot \cos\varphi - \sin\varphi}{\sqrt{\left(\frac{b}{\varphi}\right)^2 + 1}} \right) \tag{19}$$

Where

x_{21} is x-coordinate of the outer wall of the second gap [m]

y_{12} is x-coordinate of the outer wall of the second gap [m]

The inner wall of the second (mirror image) gap has the equations

$$x_{22} = \left(x_2 - \frac{c}{2} \cdot \frac{\left(\frac{b}{\varphi}\right) \cdot \sin\varphi + \cos\varphi}{\sqrt{\left(\frac{b}{\varphi}\right)^2 + 1}} \right) \tag{20}$$

$$y_{22} = \left(y_2 + \frac{c}{2} \cdot \frac{\left(\frac{b}{\varphi}\right) \cdot \cos\varphi - \sin\varphi}{\sqrt{\left(\frac{b}{\varphi}\right)^2 + 1}} \right) \tag{21}$$

Where

x_{12} is x-coordinate of the inner wall of the first gap [m]

y_{12} is x-coordinate of the inner wall of the first gap [m]

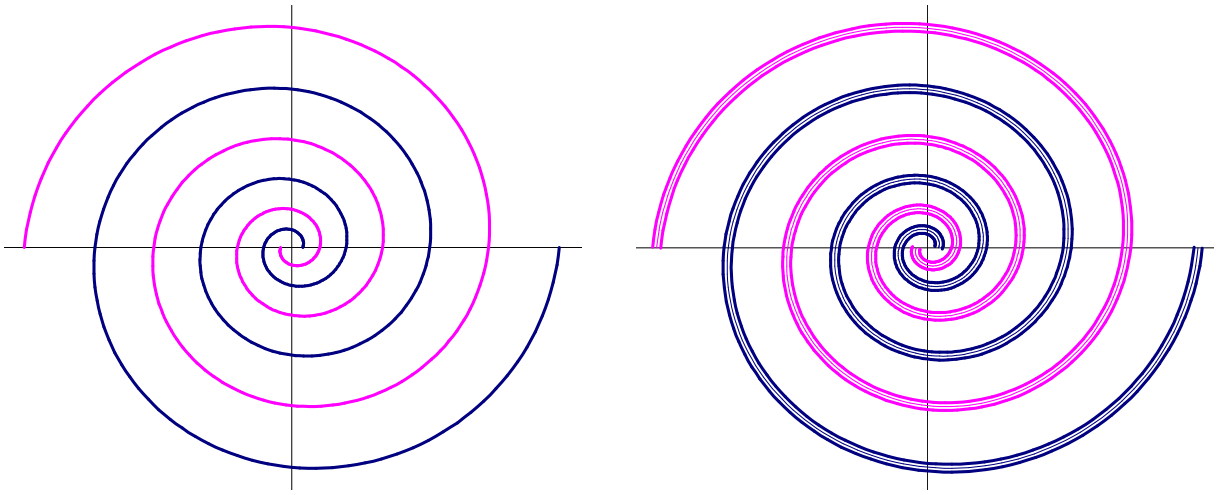

Fig. 3: Centerline of the gap spiral and its mirror image (left), gap and its mirror image (right)

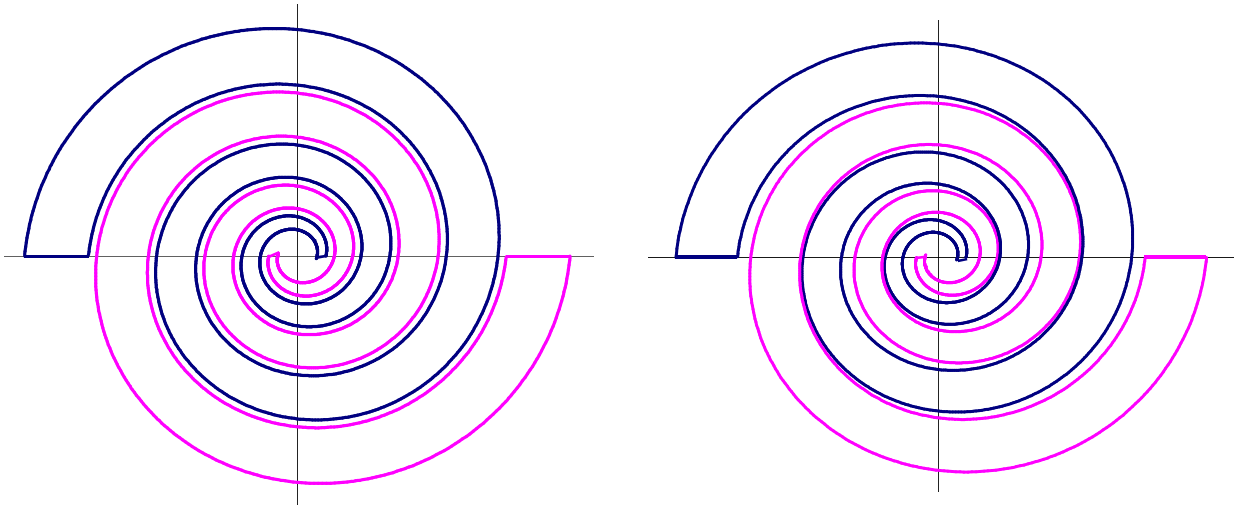

Fig. 4: Centered fixed and orbiting vanes (left), engaged vanes (right)

On the left in Fig. 3, we can see both centerlines, and on the right in Fig 3, we can see two symmetrical gaps that are centered at the common origin of the x-y system of coordinates.

In the Fig 3, we can see that the vanes (scrolls) are created by the space between gaps. The outer wall of the first gap and the inner wall of the second gap will form one vane, and the inner wall of the first gap and the outer wall of the second gap will create second vane. This may be seen in the Fig. 4. By comparing Fig. 3 and Fig 4, we can also see that certain parts of each vane, at the center and on the circumference, are cut off, because they are not needed.

2.2 Built-in Compression Ratio

The scroll compressor is a constant pressure ration machine. Assuming polytropic compression, the gas that is taken into the suction pocket is discharged out from the discharge pocket at the pressure that is equal to

$$p_D = p_S \cdot C_R^n \tag{22}$$

Where

p_S is suction pressure [Pa]
p_D is discharge pressure [Pa]
n is polytropic coefficient

The built-in compression ratio is the ratio of the volume of suction pocket to the volume of the discharge pocket. Because the volume of a pocket is equal to the area of the pocket multiplied by the constant height of vane, we can consider only the area of each pocket.

$$C_R = \frac{V_D}{V_S} = \frac{A_D \cdot h}{A_S \cdot h} = \frac{L_D \cdot c}{L_S \cdot c} = \frac{L_D}{L_S} \tag{23}$$

Where

V_D is volume of discharge pocket [m^3]
V_S is volume of suction pocket [m^3
A_D is area of suction pocket [m^2]
A_S is area of discharge pocket [m^2]
L_D is length of the centerline of discharge pocket [m]
L_S is length of the centerline of suction pocket [m]
h is height of vane [m]

Equation (23) shows that the built-in compression ratio is the ratio of the length of centerline of the discharge gas to the length of the centerline of the suction gap.

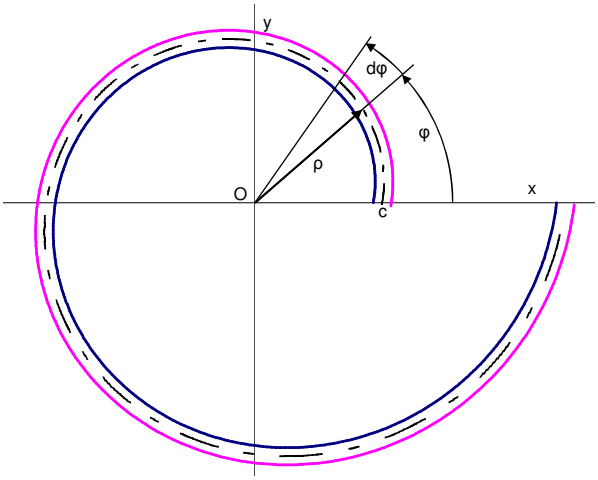

Fig. 5: Area of a pocket

The length L of the centerline of the gap between scrolls is always equal to the length of an arc that has angle from φ to φ + 2π.

$$L = \int_{\varphi_1}^{\varphi_2} \rho(\varphi) \cdot d\varphi \tag{25}$$

In the case of a power spiral we have

$$L = a \cdot \int_{\varphi_1}^{\varphi_2} \varphi^b \cdot d\varphi = a \cdot \left[\frac{\varphi^{b+1}}{b+1} \right]_{\varphi_1}^{\varphi_2} \tag{26}$$

The result obtained from equation (25) has sufficient engineering accuracy and the integration is not difficult. If we wish, we can use formulae that are more precise

$$L = \int_{\varphi_1}^{\varphi_2} \sqrt{x'^2(\varphi) + y'^2} \cdot d\varphi = \int_{\varphi_1}^{\varphi_2} \sqrt{\rho^2(\varphi) + \rho'^2(\varphi)} \cdot d\varphi \tag{27}$$

In the case of a power spiral the result of integration of any expression in (27) depends on the value of exponent b, and the integration may not be easy.

The advantage of power spiral over the involute of a circle is in that that the power spiral can achieve higher built-in compression ratio. For example, the compressor with scrolls that are involutes of a circle has built-in compression ratio 1.66 on the working angle 2π, while the compressor with power scrolls has built-in compression ratio 2.71 on the same working angle.

While we can change the built-in compressor ratio of an involute of a circle based compressor by increasing working angle, we can change the built-in compression ratio of a power spiral based compressor by changing exponent b while keeping working angle constant.

2.3 Contact Between Mating Scrolls

Contact between mating scrolls is an important property of the scroll compressor. The reactions between mating scrolls of a scroll compressor based on the involute of a circle have direction that is tangent to both generating radii and thus identical with the direction of the orbiting radius. In the contrary, the reactions between mating scrolls of a scroll compressor based on the power spiral do not have any reaction between mating scrolls parallel with the orbiting radius. As a matter of fact, the reaction at each contact point passes through that point and the center of curvature that is on the locus of centers of curvature. The center of curvature of a plane curve has the coordinates

$$x_C = \rho \cdot \cos\varphi - \frac{\left(\rho^2 + \left(\frac{d\rho}{d\varphi} \right)^2 \right) \cdot \left(\rho \cdot \cos\varphi + \frac{d\rho}{d\varphi} \cdot \sin\varphi \right)}{\rho^2 + 2 \cdot \left(\frac{d\rho}{d\varphi} \right)^2 - \rho \cdot \frac{d^2\rho}{d\varphi^2}} \tag{28}$$

$$y_C = \rho \cdot \sin\varphi - \frac{\left(\rho^2 + \left(\frac{d\rho}{d\varphi} \right)^2 \right) \cdot \left(\rho \cdot \sin\varphi - \frac{d\rho}{d\varphi} \cdot \cos\varphi \right)}{\rho^2 + 2 \cdot \left(\frac{d\rho}{d\varphi} \right)^2 - \rho \cdot \frac{d^2\rho}{d\varphi^2}} \tag{29}$$

Thus, for the value of b = 2, and after we find all derivatives of equation (5), locus of centers of curvature has coordinates

$$x_C = a \cdot \left[\varphi^2 \cdot \left(1 - \frac{\varphi^4 + 4}{\varphi^2 + 6} \right) \cdot \sin\varphi + \frac{2 \cdot \varphi \left(\varphi^2 + 4 \right)}{\varphi^2 + 6} \cdot \cos\varphi \right] \tag{30}$$

$$y_C = a \cdot \left[\varphi^2 \cdot \left(1 - \frac{\varphi^4 + 4}{\varphi^2 + 6} \right) \cdot \cos\varphi - \frac{2 \cdot \varphi \left(\varphi^2 + 4 \right)}{\varphi^2 + 6} \cdot \sin\varphi \right] \tag{31}$$

Equations (30) and (31) represent another spiral. This indicates that the normal reactions change their directions. The change in the direction of normal reaction may generate more harmonic components and thus will contribute to generation of vibration and noise. Fig. 6 is an example of the locus of centers of curvature of the spiral in Fig. 4.

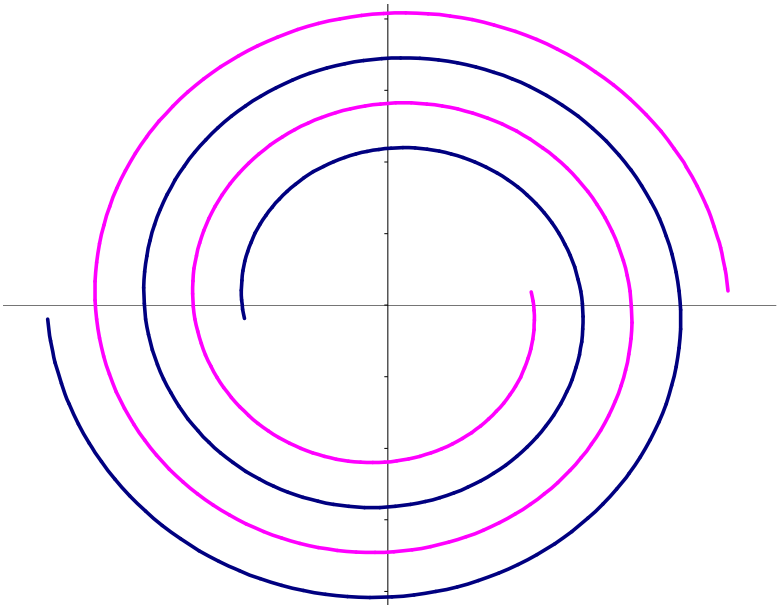

Fig. 6: Locus of centers of curvature

3. CONCLUSIONS

The theory of parallel curves enables design of scroll compressors with vanes that are other types of plane spirals. It can be seen that spirals, which radius vector increases linearly, such as the involute of a circle and Archimedes spiral, can form pairs of symmetrical pockets, and that the thickness of vanes is constant. Other types of spirals such as power spirals, which radius vector increases nonlinearly also form pairs of symmetrical pocket, but the thickness of vanes increases with increasing radius vector. Power spirals can achieve higher built-in compression ratio in the same working angle than the involute of a circle.

REFERENCES

Gravesen, J., Henriksen, C.,2001, The Geometry of the Scroll Compressor, *SIAM Review*, Vol. 43, No. 1, pp 113-126.

Rektorys, K., 1969, Survey of Applicable Mathematics, *MIT Press*.